2017

Salsalate treatment following traumatic brain injury reduces inflammation and promotes a neuroprotective and neurogenic transcriptional response with concomitant functional recovery

Mouna Lagraoui
Uniformed Services University

Gauthaman Sukumar
Uniformed Services University

Joseph R. Latoche
Uniformed Services University

Sean K. Maynard
Uniformed Services University

Clifton L. Dalgard
Uniformed Services University

See next page for additional authors

Authors
Mouna Lagraoui, Gauthaman Sukumar, Joseph R. Latoche, Sean K. Maynard, Clifton L. Dalgard, and Brian C. Schaefer

Brain, Behavior, and Immunity 61 (2017) 96–109

Contents lists available at ScienceDirect

Brain, Behavior, and Immunity

journal homepage: www.elsevier.com/locate/ybrbi

Full-length Article

Salsalate treatment following traumatic brain injury reduces inflammation and promotes a neuroprotective and neurogenic transcriptional response with concomitant functional recovery

Mouna Lagraoui [a,b], Gauthaman Sukumar [b,c], Joseph R. Latoche [a,b,1], Sean K. Maynard [a,b,2], Clifton L. Dalgard [b,c], Brian C. Schaefer [a,b,*]

[a] Department of Microbiology and Immunology, Uniformed Services University, Bethesda, MD, USA
[b] Center for Neuroscience and Regenerative Medicine, Uniformed Services University, Bethesda, MD, USA
[c] Department of Anatomy, Physiology, and Genetics, Uniformed Services University, Bethesda, MD, USA

ARTICLE INFO

Article history:
Received 8 August 2016
Received in revised form 18 November 2016
Accepted 6 December 2016
Available online 7 December 2016

Keywords:
TBI
Myeloid cells
Microglia
NF-kappaB
Salicylate
Neuroprotection
Neuroregeneration
Oxytocin
Motor function
NSAID

ABSTRACT

Neuroinflammation plays a critical role in the pathogenesis of traumatic brain injury (TBI). TBI induces rapid activation of astrocytes and microglia, infiltration of peripheral leukocytes, and secretion of inflammatory cytokines. In the context of modest or severe TBI, such inflammation contributes to tissue destruction and permanent brain damage. However, it is clear that the inflammatory response is also necessary to promote post-injury healing. To date, anti-inflammatory therapies, including the broad class of non-steroidal anti-inflammatory drugs (NSAIDs), have met with little success in treatment of TBI, perhaps because these drugs have inhibited both the tissue-damaging and repair-promoting aspects of the inflammatory response, or because inhibition of inflammation alone is insufficient to yield therapeutic benefit. Salsalate is an unacetylated salicylate with long history of use in limiting inflammation. This drug is known to block activation of NF-κB, and recent data suggest that salsalate has a number of additional biological activities, which may also contribute to its efficacy in treatment of human disease. Here, we show that salsalate potently blocks pro-inflammatory gene expression and nitrite secretion by microglia in vitro. Using the controlled cortical impact (CCI) model in mice, we find that salsalate has a broad anti-inflammatory effect on in vivo TBI-induced gene expression, when administered post-injury. Interestingly, salsalate also elevates expression of genes associated with neuroprotection and neurogenesis, including the neuropeptides, oxytocin and thyrotropin releasing hormone. Histological analysis reveals salsalate-dependent decreases in numbers and activation-associated morphological changes in microglia/macrophages, proximal to the injury site. Flow cytometry data show that salsalate changes the kinetics of CCI-induced accumulation of various populations of CD11b-positive myeloid cells in the injured brain. Behavioral assays demonstrate that salsalate treatment promotes significant recovery of function following CCI. These pre-clinical data suggest that salsalate may show promise as a TBI therapy with a multifactorial mechanism of action to enhance functional recovery.

Published by Elsevier Inc.

1. Introduction

TBI is a major cause of morbidity and mortality throughout the world, with resultant healthcare costs representing a huge economic burden for developed countries (Fu et al., 2016). However, despite decades of basic research and clinical studies, there is not yet an accepted therapy for TBI, and treatment remains limited to supportive care. There thus remains an urgent need to identify novel therapeutics for this devastating class of injuries.

Neuroinflammation plays a central role in the pathophysiology of TBI. Tissue damage and destruction following TBI involves both the primary injury, in which brain tissue is directly damaged by the physical insult, and a secondary injury, in which direct tissue damage is further amplified by a variety of consequent processes, including tissue necrosis, ischemia, and activation of the inflammatory cascade (Hellewell et al., 2015; Kumar and Loane, 2012).

* Corresponding author at: Department of Microbiology and Immunology, Uniformed Services University, 4301 Jones Bridge Road, Bethesda, MD 20814, USA.
E-mail address: brian.schaefer@usuhs.edu (B.C. Schaefer).
[1] Present address: Integrative Cardiac and Metabolic Health Program, Windber Research Institute, 620 7th Street, Windber, PA 15963, USA.
[2] Present address: MedImmune, One MedImmune Way, #2214F Gaithersburg, MD 20878, USA.

http://dx.doi.org/10.1016/j.bbi.2016.12.005
0889-1591/Published by Elsevier Inc.

Among the cellular components of the neuroinflammatory response post-TBI, microglia and astrocytes play a prominent role in the induction and regulation of inflammation. Microglia are CNS-resident myeloid lineage cells which serve as immune sentinels, as well as playing many other roles in CNS physiology (Marin and Kipnis, 2016; Tay et al., 2016). Upon activation by endogenous "danger" signals produced by damaged or necrotic cells, microglia release numerous pro-inflammatory mediators including cytokines, chemokines, reactive oxygen species (ROS) and nitric oxide (NO) (DeLegge and Smoke, 2008; Kettenmann et al., 2011; Qin et al., 2007). Astrocytes also undergo phenotypic changes in response to TBI, increasing in size, upregulating production of glial fibrillary acidic protein (GFAP) and vimentin, and releasing inflammatory mediators (Gorina et al., 2011; Paintlia et al., 2013; Sofroniew and Vinters, 2010; Zamanian et al., 2012).

Surprisingly, data suggest that the post-TBI inflammatory response can persist for decades in humans (Smith et al., 2013). Evidence is accumulating that persistent neuroinflammation after TBI is a major driver of neurodegeneration (Faden and Loane, 2015). Given the extended time scale of inflammation-induced tissue injury, the reduction of neuroinflammation is a particularly important intervention strategy to limit TBI-driven tissue destruction. Indeed, considerable effort is being directed towards the development of therapeutics to ameliorate neuroinflammation (Hellewell et al., 2015). To date, however, trials of various candidate anti-inflammatory therapies have not yielded compelling evidence of clinical benefit in TBI.

Many now argue that TBI is too biologically complex to treat successfully by targeting a single aspect of the injury-induced pathology (Loane et al., 2015; Margulies et al., 2009; Stoica et al., 2009; Vink and Nimmo, 2009). In this respect, it would be desirable to identify candidate TBI therapeutics that both reduce inflammation and possess other biological activities that mitigate damage and promote a successful healing response.

The transcription factor NF-κB is a primary driver of the host immune response, including the inflammatory cascade (Vallabhapurapu and Karin, 2009). Our previous work has demonstrated a prominent NF-κB transcriptional signature, including many inflammation-associated gene products, following both minor and severe brain injury (Lagraoui et al., 2012). Thus, a logical approach to limit TBI-dependent inflammation would be to inhibit NF-κB activation, post-injury. We therefore sought to identify FDA-approved drugs that are known to inhibit NF-κB activation and to cross the blood-brain barrier (BBB). One such drug meeting these criteria is salsalate, a non-steroidal anti-inflammatory drug (NSAID), which, like aspirin, is a salicylate. Salicylate-based drugs have a long history of clinical application (Hedner and Everts, 1998). A key distinction between salsalate and aspirin is that salsalate is a non-acetylated salicylate. Acetylated salicylates, including aspirin, irreversibly inactivate cyclooxygenase (COX) enzymes, which accounts for their potent inhibition of the clotting cascade. Lacking this acetyl group, salsalate is a weak and reversible COX inhibitor, which does not have significant anti-coagulant activity (Marnett, 2009). However, like aspirin, salicylate (the metabolized product of salsalate) potently suppresses NF-κB activation through inhibition of the enzymes IκB kinase (IKK)-α and IKK-β (Kopp and Ghosh, 1994; Pierce et al., 1996; Yin et al., 1998). Moreover, recent studies demonstrate that salsalate (and/or salicylate) has several other biological activities independent of effects on the NF-κB pathway, with at least one activity that appears to protect against neurodegeneration (Hawley et al., 2012; Min et al., 2015; Shirakawa et al., 2016). Thus, salsalate may have the desired multimodal mechanism of action to be considered a candidate TBI therapy.

In this study, we investigated the therapeutic efficacy of salsalate treatment for TBI, using the well-established CCI model in mice. We first demonstrated that salsalate potently inhibits inflammatory gene expression and functional responses in a microglia cell line, confirming that salsalate is capable of inhibiting a cell population which plays a central role in the CNS inflammatory response (Karve et al., 2016). Then, employing the CCI model, we used an unbiased transcriptomics approach to demonstrate that the primary effect of salsalate on TBI-induced transcription is suppression of a gene set that is highly enriched in NF-κB-regulated mediators of inflammation. However, salsalate also modestly induced a cohort of genes. This induced subset is nearly devoid of pro-inflammatory genes, and highly enriched in known mediators of neuroprotection and neurogenesis. Of particular interest in the induced subset were the transcripts encoding the neuropeptides oxytocin and thyrotropin releasing hormone, both of which are known to mediate protective effects in TBI. We furthermore performed histological analysis of glial expansion, finding a significant reduction in the population of activated microglia/macrophages at the injury site, with a possible reduction in activated astrocytes, providing further evidence of salsalate-mediated suppression of the inflammatory response. In addition, flow cytometry data demonstrated that salsalate treatment altered kinetics of accumulation of distinct populations of infiltrating blood leukocytes in the injured brains. Assays of motor function revealed that salsalate treatment promotes significant recovery during the week post-injury. Together, these data suggest that salsalate promotes recovery from traumatic brain injury via both inhibition of inflammation and induction of a gene expression program associated with neuroprotection and neurogenesis. The potential multifactorial mode of protection suggests that salsalate may be particularly promising as a therapeutic candidate for the treatment of human TBI.

2. Materials and methods

2.1. BV2 cell culture and gene expression assays

The murine microglia line, BV-2 (Blasi et al., 1990), was cultured in DMEM supplemented with 10% FBS and 1% pen/strep at 37 °C in a humidified incubator with 5% CO_2. Cells were seeded in 6-well plates at a density of 5×10^5 cells/well. After overnight incubation, the culture medium was changed, and cells were pretreated with salsalate (0.5, 1, 2, and 3 mM) or vehicle (1xPBS) for 1 h, followed by stimulation with 0.5 μg/ml LPS. After 24 h of LPS stimulation, supernatant was collected and stored at −20 °C and cells were processed for RNA isolation. RT-PCR was performed as described below.

2.2. Nitrite measurement

BV2 microglia cells were cultured overnight in 6 well plates in a density of 5×10^5 cells/well and pretreated with salsalate (0.5, 1, 2, and 3 mM) or vehicle for 1 h, then stimulated with 0.5 μg/ml LPS or vehicle (1 × PBS) for 24 h. After incubation, the culture medium was collected and stored at −20 °C until performance of the assay. Release of nitric oxide was quantified by measuring the stable metabolite, nitrite, using a Nitrate/Nitrite assay kit (Sigma, St. Louis, MO), according to the manufacturer's instructions.

2.3. Animals and surgical procedures

Ten- to twelve-week old C57BL/6 male mice were subjected to TBI using an Impact One™ Stereotaxic Impactor (myNeuroLab, St. Louis, MO, USA), as we have previously described (Lagraoui et al., 2012). Briefly, mice were anesthetized with 2% isoflurane in 98% oxygen, followed by positioning in a stereotaxic frame. Craniotomy

was performed over the left hemisphere using a hand-held 5 mm trephine over the motor cortex (1.8 mm medial-lateral, 2 mm from Bregma). Mice were then subjected to CCI using a 3 mm flat-tip with a velocity of 5 m/s at a depth of 2.0 mm for 200 ms. After trauma, the craniotomy was closed with the previously removed bone and bone wax, and the incision was closed with sutures. Naïve mice were anesthetized with 2% isoflurane in 98% oxygen, monitored until recovery from anesthesia, and transferred to fresh cages. Animals were not treated (naïve) or *i.p.* injected with 50 mg/kg salsalate (Alfa Aesar, MA) or vehicle (DMSO-PBS) 30 min post-CCI and once daily for five consecutive days. The Institutional Animal Care and Use Committee at Uniformed Services University (USU) approved all animal procedures.

2.4. Tissue harvesting and RNA extraction

Animals were sacrificed on day +3 post-CCI for transcriptome profiling and real-time PCR experiments. Mice were perfused with 1 × PBS and brains were removed from the skull. A 5 mm diameter punch biopsy encompassing the exact injury site on the left hemisphere was collected from each CCI animal. The equivalent region was collected from control (naïve) animals. The depth of the punch was approximately 5 mm. RNA extraction from both in vitro cell cultures and biopsy tissue was via the guanidinium isothiocyanate-phenol extraction method (Chomczynski and Sacchi, 1987).

2.5. Transcriptome profiling by RNA sequencing

Total RNA was quantified via a fluorescence dye-based methodology (RiboGreen) on a Spectramax Gemini XPS plate reader (Molecular Devices, Mountain View, CA). RNA integrity was assessed using gel-based electrophoresis on an Experion Automated Electrophoresis System (Bio-Rad, Hercules, CA). Total RNA input of 200 ng was used for library preparation using the TruSeq Stranded mRNA Library Preparation Kit (Illumina, San Diego, CA). Sequencing libraries were quantified by PCR using KAPA Library Quantification Kit for NGS (Kapa, Wilmington, MA) and assessed for size distribution on an Experion Automated Electrophoresis System. Sequencing libraries were pooled and sequenced on a NextSeq 500 Desktop Sequencer (Illumina) using a NextSeq 500 High Output Kit v2 with paired-end reads at 75 bp length. Raw sequencing data was demuxed using bcl2fastq2 Conversion Software 2.17 before alignment using TopHat Alignment v1.0 and differential expression analysis using Cufflinks Assembly & DE v1.1.0 on BaseSpace Onsite (Illumina).

2.6. Real-time PCR analyses

RNA samples (2 μg) were reverse transcribed to cDNA, using random hexamers and Superscript II Reverse Transcriptase (Life Technologies, Carlsbad, CA, USA), in a 1 h reaction at 42 °C. Real-time PCR analysis of cDNA was performed using an RT-PCR master mix for TaqMan assays (SydLabs, Inc., Malden, MA, USA) and an iQ5 instrument (Bio-Rad, Hercules, CA, USA) in 96-well format with 20 μl reaction volume per well. Primers for TaqMan assays were designed using Primer Express 3.0 software (Life Technologies, Carlsbad, CA, USA) or a web based RealTime qPCR Assay design platform (Integrated DNA Technologies, Coralville, IA). PCR primers and FAM-ZEN-Iowa Black double-quenched probes were purchased from Integrated DNA Technologies (Coralville, IA, USA). Primer sequences are listed in Table 1. GAPDH was used as a normalization control for all probe sets.

The delta Ct (ΔC_t) method was used for PCR array data analysis. The normalized ΔC_t for each gene of interest (GOI) was calculated by deducting the C_t of the housekeeping gene (HKG: GAPDH) from

Table 1
Real-time PCR primers.

IL-1β	
Sense	
GAGCACCTTCTTTTCCTTCATCTT	
anti-sense	
CACACACCAGCAGGTTATCATCA	
Probe	
AGAAGAGCCCATCCTCTGTGACTCATGG	
Tnf-α	
Sense	
GGTCCCCAAAGGGATGAGAA	
anti-sense	
TGAGGGTCTGGGCCATAGAA	
Probe	
TTCCCAAATGGCCTCCCTCTCATCA	
Ccl2	
Sense	
GGCTCAGCCAGATGCAGTTAA	
anti-sense	
CCTACTCATTGGGATCATCTTGCT	
Probe	
CCCCACTCACCTGCTGCTACTCATTCA	
Ccl5	
Sense	
GGGTACCATGAAGATCTCTGC	
anti-sense	
GCGAGGGAGAGGTAGGCAAAG	
Probe	
TGAGGATGATGGTGAGGGCAGC	
Cxcl10	
Sense	
TCAGCACCATGAACCCAAG	
anti-sense	
CTATGGCCCTCATTCTCACTG	
Probe	
TGCCGTCATTTTCTGCCTCATCCT	
MMP13	
Sense	
TTGATGCCATTACCAGTCTCC	
anti-sense	
ACATGGTTGGGAAGTTCTGG	
Probe	
AGCAGGTTGAGGCTGAGCTCTTT	
MNDA	
Sense	
CCAGTCACCAATACTCCACAG	
anti-sense	
GAGCACCATCACTGTCAGG	
Probe	
AACCCCAGAACCAGAACATTCCCA	
Eomes	
Sense	
CACCCAGAATCTCCTAACACTG	
anti-sense	
AGCCTCGGTTGGTATTTGTG	
Probe	
AAATCTCCTGCCTCATCCAGTGGG	
Oxytocin	
Sense	
TGCTTGGCTTACTGGCTC	
anti-sense	
GCAGATGCTTGGTCCGAAG	
Probe	
CCTCGGCCTGCTACATCCAGAAC	
Lhx8	
Sense	
ACAGTTCGCTCAGGACAAC	
anti-sense	
AAGAATGGTTGGGACTGACG	
Probe	
AGAAACTGGCAGAAAGGACAGGCT	

GAPDH
Sense
TGTGTCCGTCGTGGATCTGA
anti-sense
CCTGCTTCACCACCTTCTTGA
Probe
CCGCCTGGAGAAACCTGCCAAGTATG

the C_t of each GOI: $\Delta C_t = (Ct^{GOI} - Ct^{HKG})$. The $\Delta\Delta$Ct for each GOI was calculated by deducting the average ΔC_t of GOI in the naïve group from the ΔC_t of each GOI in the CCI group: $\Delta\Delta C_t = \Delta C_t$ (CCI group) – average ΔC_t (naïve group). The fold-change of each GOI compared to the naïve group was calculated as: Fold-change = $2^{(-\Delta\Delta Ct)}$.

2.7. Histology

For immunofluorescence microscopy analysis, mice (6 animals per group) were sacrificed at day +7 following CCI. Brains were perfused with cold PBS then with 4% paraformaldehyde. Brains were dissected from the animal and incubated in 4% paraformaldehyde for 8–10 h, followed by transfer to a solution of 30% sucrose, with incubation at 4 °C for 14 to 16 h. Brains were then frozen in Tissue-Tek OCT (Sakura Finetek, Torrance, CA, USA) and stored at −80 °C. Coronal cryosections (20 μm) were collected and stored at −80 °C until immunostaining. Astrocytes were identified by staining with an AlexaFluor 555-conjugated GFAP Mouse monoclonal antibody (Cell Signaling Technology; Danvers, MA). Microglia were detected via staining with a Rabbit anti-Iba1 polyclonal antibody (Wako Chemicals USA; Richmond, VA) using an Alexa-Fluor 488 Goat anti-Rabbit IgG secondary reagent (Thermo Fisher Scientific; Waltham, MA). Slides were examined using a fluorescent microscope (Leica DM5500 B), employing a 40× objective. GFAP and Iba-1 immunostained brain sections were analyzed using ImageJ software to quantify the intensity for each image. A cell counter plugin for ImageJ was used to determine cell number per unit area.

2.8. Flow cytometry

On days +3 and +7 post-CCI, mice (4 per treatment condition) were sacrificed and brains were collected and processed for flow cytometry. Briefly, mice were perfused with 1 × PBS and brains were harvested and digested with collagenase III (Worthington Biochemical, Lakewood, NJ) and dispase (Roche, via Sigma-Aldrich, St Louis, MO). Cells were isolated using a 70%, 37%, 30% Percoll gradient (GE-Healthcare Biosciences, via Sigma-Aldrich, St Louis, MO) in 1 × PBS solution. After isolation, cells were treated with anti-Fc block and stained with the following antibodies: V450 anti-CD45.2, PerCP-Cy5.5 anti-CD11b, FITC anti-Ly6G, and BV605 anti-Ly6C (BD Biosciences, San Jose, CA). After staining, cells were washed, fixed, and analyzed using an LSR II cytometer (BD Biosciences, San Jose, CA) and FlowJo 10.2 software (FlowJo, LLC, Ashland, OR).

2.9. Behavior studies

Rotarod and balance beam tests were performed (9 mice per group) on days; −1, +1, +3, and +7 relative to surgical procedures, as we have previously described (Lagraoui et al., 2012). Briefly, for rotarod testing, mice were acclimated to the apparatus (Ugo Basile, Collegeville, PA, USA) for 60 s at a fixed speed of 5 rpm. After the adaptation phase, animals were placed on the rotarod and the acceleration was increased from 5 to 60 rpm within 180 s. Latency to fall from the accelerating rotarod and the maximal attained speed were recorded for each mouse. Three trials were performed for each animal and the average was recorded. For balance beam testing, mice were placed on a narrow beam (0.5 cm) and trained to cross the beam for three consecutive days before the first test. On the testing day, the mice were placed on the beam and the time spent to cross and the number of foot-slips occurring during the beam cross were recorded. Three trials were performed for each animal and the average was calculated. The beam cross score was calculated using the formula: (F/C) × T, where F = number of foot slips, C = length of beam (80 cm) and T = time spent to cross the beam.

2.10. Statistical analyses

For in vitro experiments (RT-PCR and Nitrite release), one-way ANOVA with Dunnett's multiple comparisons test was used to determine significance. For in vivo experiments (CCI), the Mann-Whitney *U* test was used to analyze Real-time PCR results; one-way analysis of variance (ANOVA) with Tukey's multiple comparisons test was used to analyze GFAP and Iba1 histology results; two-way ANOVA with Tukey's multiple comparisons test was used to analyze flow cytometry data; two-way ANOVA with Tukey's multiple comparisons test (within groups) and Sidak's multiple comparisons test (between groups) was used for behavior data statistics. A p value <0.05 was considered statistically significant.

3. Results

3.1. In vitro inhibition of microglia proinflammatory responses by salsalate treatment

Salsalate has previously been demonstrated to potently inhibit NF-κB signaling through blocking activation of both IKKα and IKKβ (Kopp and Ghosh, 1994; Pierce et al., 1996; Yin et al., 1998). As the production of pro-inflammatory cytokines is highly dependent on intact IKKβ activity, we predicted that salsalate treatment would block stimulus-dependent production of pro-inflammatory mediators by sentinel immune cells in the CNS. To provide in vitro data to directly support this prediction, we pretreated the murine microglia cell line, BV2, with a range of concentrations of salsalate, from 0.5 mM to 3 mM. BV2 cells were then stimulated with the TLR4 agonist, bacterial lipopolysaccharide (LPS), to induce transcription of NF-κB-dependent proinflammatory cytokines. As shown in Fig. 1A, all four doses of salsalate potently inhibited LPS-dependent transcription of IL-1β and TNF-α, two key pro-inflammatory cytokines. We also analyzed the effect of salsalate pre-treatment on an inflammation-associated microglia functional response, the secretion of nitrite. As shown in Fig. 1B, we observed a dose-dependent decrease in LPS-stimulated secretion of nitrite in BV2 cells which had been pretreated with escalating amounts of salsalate. Together, these data show that salsalate pretreatment substantially inhibits NF-κB-dependent inflammatory responses of microglia in vitro.

3.2. Salsalate treatment reduces expression of proinflammatory genes and increases expression of genes associated with neuroprotection and/or neurogenesis

As data suggest that microglia play a key role in initiating and maintaining the inflammatory response to TBI (Loane and Byrnes, 2010), the data in Fig. 1 suggested that salsalate treatment may be useful for modulating such responses in vivo. To assess the in vivo therapeutic efficacy of salsalate as a TBI therapy, we utilized the mouse CCI model, in which we have previously shown that injury induces both a strong NF-κB-dependent inflammatory response and a significant impairment of motor function, which

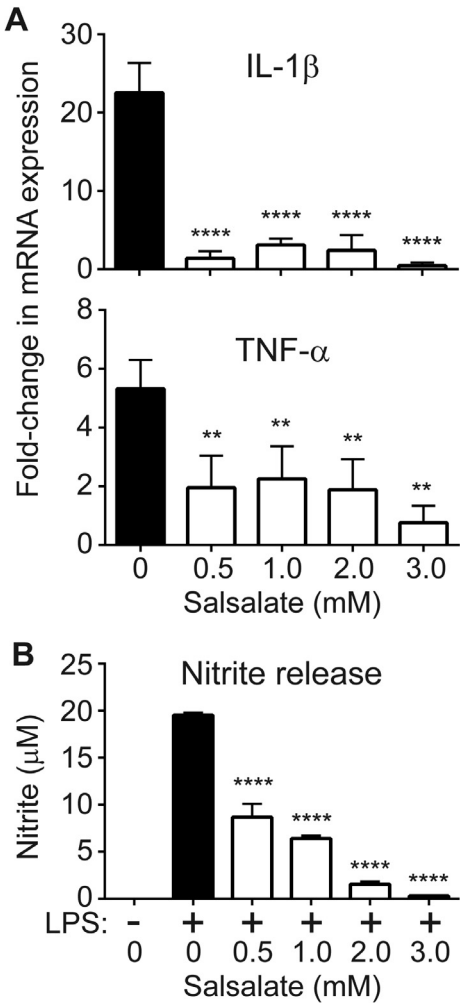

Fig. 1. Salsalate treatment of the BV2 microglia cell line inhibits LPS-induced inflammatory responses. (A) TaqMan real-time PCR analysis of salsalate-mediated repression of LPS-stimulated IL-1β and TNF-α gene expression in BV2 microglia cells. (B) Quantification of nitrite release by untreated and salsalate-treated BV2 microglia cells, following LPS treatment. $^{****}p < 0.0001$ and $^{**}p < 0.01$, one-way ANOVA with Dunnett's multiple comparisons test.

recovers to pre-injury levels by day +7 post-injury (Lagraoui et al., 2012).

Mouse CCI experiments included three groups: naïve (no CCI, no treatment), vehicle (CCI, DMSO treatment) and salsalate (CCI, salsalate treatment). Administration of salsalate was once per day for five days, starting 30 min post-injury. In a previous study of CCI-induced inflammation, we found peak induction of the majority of inflammatory genes occurred by day +3 post-injury (Lagraoui et al., 2012). Thus, we chose a five day drug administration time course to encompass this acute phase of post-CCI inflammation. For initial salsalate administration, we chose the 30 min post-injury time point, as we considered this a reasonable model for administration of therapeutic intervention following acute human TBI. Although salsalate is administered to human patients via oral ingestion, oral gavage of salsalate at 30 min post-CCI injury would require considerable manipulation of animals while in a fragile post-injury state. We therefore delivered salsalate via intraperitoneal injection, which can be performed rapidly with minimal handling of injured mice. Salsalate is processed to salicylic acid via the action of a broad class of aryl hydrolases which are expressed in all tissues, with abundant presence in the blood. Indeed, much processing of ingested salsalate occurs in the blood (Cao et al., 2012; Harrison et al., 1981). Thus, IP-administered salsalate should be processed rapidly to salicylic acid. Moreover, systemic release of salicylic acid is likely to be more rapid by injection than via gavage/ingestion, because transit through the acidic environment of the stomach (where no processing occurs) is avoided.

For initial assessment of the effects of salsalate treatment on the response to TBI, we employed an unbiased transcriptomics approach, using a small cohort of animals (4 per treatment group). We chose day +3 as our analysis time point, since our previous analysis of the inflammatory response to CCI demonstrated that day +3 is the peak of expression for many inflammatory transcripts, with significant elevation of expression for most other inflammation-associated transcripts that we analyzed (Lagraoui et al., 2012). As anticipated (Fig. 2A), we observed a high asymmetry of injury-associated differential gene expression in the CCI-vehicle group as compared to the naïve experimental group (1425 genes induced versus 105 genes repressed, at greater than 2-fold ratio in expression), consistent with our previous analysis by BeadArray RNA expression profiling (Lagraoui et al., 2012). Of the gene set with increased expression in the CCI-vehicle group, 411 of the 1425 genes are enriched for association with innate immune responses to cellular stress (p-value = 1.06e−64). In comparison, the magnitude of differential gene expression in the CCI-salsalate group as compared to the CCI-vehicle is significantly reduced, with the majority of genes being repressed (81 genes induced versus 222 genes repressed). A selection of 12 inflammatory mediators with statistically significant repression is shown in Fig. 2C. By contrast, of the 81 mRNAs induced by salsalate treatment, only 3 are annotated as being mediators of inflammation (not significant, p-value = 1e0). Moreover, we also identified a set of 28 transcripts in the group with statistically significant differential expression that are well-validated as targets of NF-κB (Pahl, 1999). Importantly, 26 of 28 (93%) were downregulated by salsalate treatment (Fig. 2D), and many of these genes overlap with the set of inflammatory mediators identified in the analysis of Fig. 2C. Overall, these data are highly consistent with our in vitro data demonstrating repression of the microglia NF-κB-dependent pro-inflammatory response (Fig. 1).

Interestingly, we noted that the salsalate-induced transcripts are enriched in several classes of genes associated with neuroprotection and/or neurogenesis, with 14 significantly elevated transcripts shown in Fig. 2E. These included neurogenic transcription factors (Eomes, Lhx8), dopamine receptors (Drd1a, Drd2), receptors for retinoids (Rarb, Rxrg), and neuropeptides (Oxt, Trh, Avp). Notably, the salsalate-induced genes segregated into three distinct patterns of gene induction, with the three neuropeptides representing a distinct group with a highly uniform pattern of expression.

We next used real-time PCR analysis of RNA obtained from a larger cohort of animals (8 per group) to confirm the transcriptomics data of Fig. 2C–E. For each of the pro-inflammatory transcripts tested, we consistently observed a reduction in expression levels in salsalate-treated animals vs. vehicle-only controls, although these reductions reached statistical significance for only Tnf-α and Ccl5 (Fig. 3A). Thus, although CCI-induced pro-inflammatory gene expression is reduced in vivo by salsalate treatment, the effect is modest in comparison to the magnitude of in vitro suppression of LPS-induced pro-inflammatory gene expression in microglia (Fig. 1A).

We also performed real-time PCR analyses to confirm salsalate-dependent elevations of expression of selected genes identified in Fig. 2E. These data confirmed that expression of the oxytocin, Eomes, and Lhx8 genes are elevated by salsalate treatment, with the increase in oxytocin expression being statistically significant (Fig. 3B). These data suggest that the effect of salsalate treatment on TBI is broader than inhibition of inflammation, and that it may also induce a neuroprotective response.

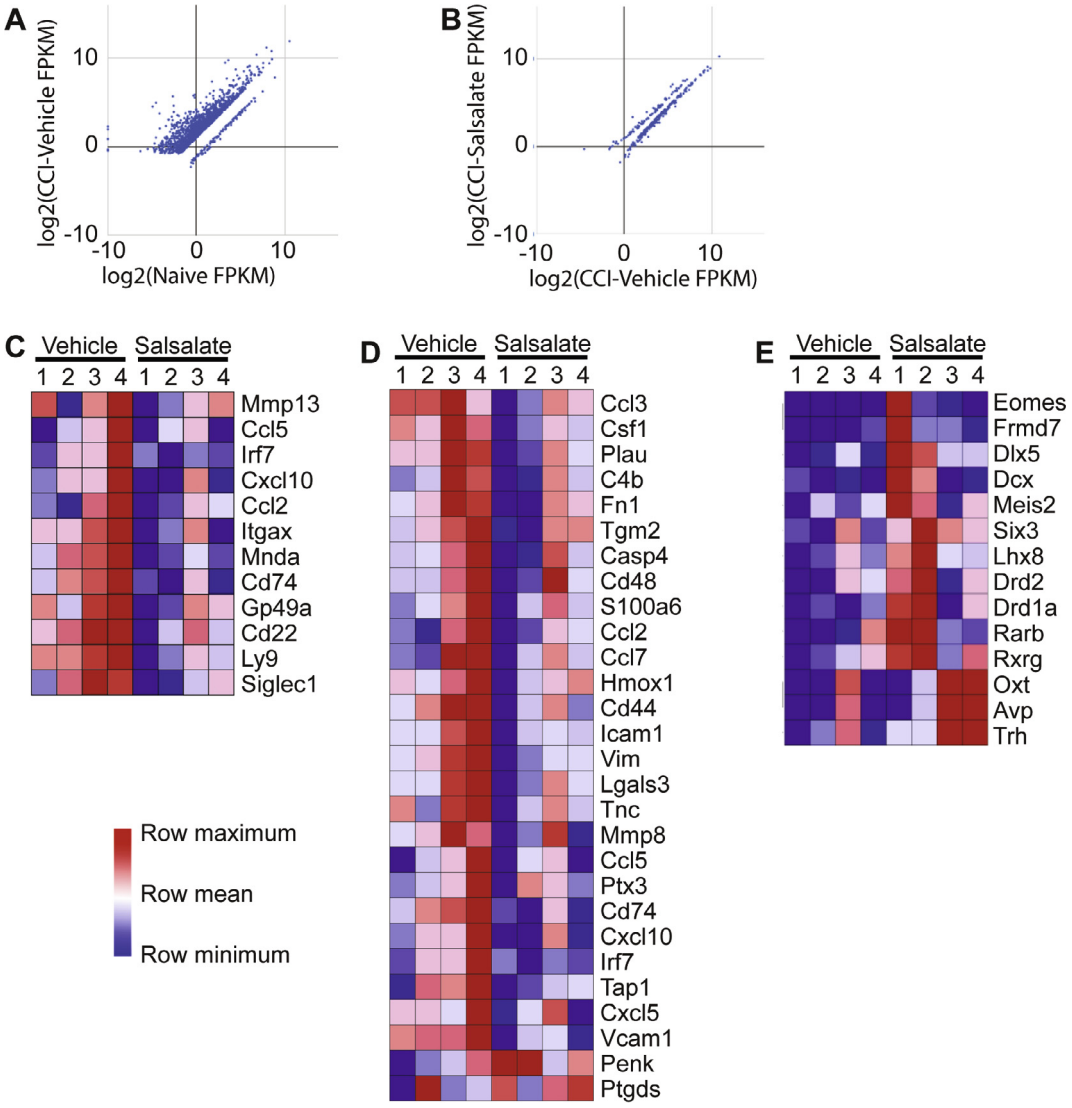

Fig. 2. Transcriptomics analyses demonstrate that salsalate inhibits proinflammatory gene expression while increasing levels of transcripts encoding neuroprotection- or neurogenesis-associated factors. (A, B) Transcriptome profiling analyses displayed as scatter plot of gene expression data normalized as fragments per kilobase of exon model per million mapped (FPKM). Plots show (A) CCI-vehicle vs. naïve (no injury) and (B) CCI-vehicle vs. CCI-salsalate. In (A), dots above the diagonal represent genes more highly expressed in the CCI-vehicle group, whereas dots below the diagonal are genes more highly expressed in naïve. In (B), dots above the diagonal represent genes more highly expressed in the CCI-salsalate group, whereas dots below the diagonal are genes more highly expressed in CCI-vehicle. (C–E) Supervised hierarchical clustering analysis heatmap showing expression of genes with statistically significant changes, as follows: (C) selected inflammatory response genes down-regulated by salsalate treatment; (D) a set of 28 NF-κB-regulated genes that were down-regulated or up-regulated by salsalate treatment; and (E) selected neurogenesis- and neuroprotection-related genes upregulated by salsalate treatment. Data were produced by RNA sequencing of injury site biopsies from 4 CCI-vehicle and 4 CCI-salsalate animals. Differential expression analysis was performed using the Cufflinks & DE Analysis algorithm on the BaseSpace Onsite (Illumina, CA) with log2ratio > 1.0 and p-value < 0.05 filters. Gene set enrichment was performed using Panther and GSEA on the GenePattern software platform (Broad Institute, MA).

To provide further evidence that salsalate activity acts beyond the NF-κB-regulated pro-inflammatory cascade, we performed a correlation analysis of a subset of genes in the above dataset. As expected, CCI-induced expression of the NF-κB-regulated pro-inflammatory gene, TNF-α, was highly correlated with other NF-κB-regulated mediators of inflammation (Ccl5, IL-1β, Ccl2), but not with expression of the oxytocin gene (Fig. 3C), which is regulated in a manner independent of NF-κB (Burbach et al., 2001; Gainer, 2012). Collectively, the data in Figs. 2 and 3 suggest that salsalate treatment of CCI-injured animals modestly represses the pro-inflammatory cascade, at least in part through its known activity as a potent NF-κB inhibitor. However, our data also suggest a previously unrecognized activity of salsalate: increasing transcription of a number of genes associated with neuroprotection and neurogenesis. Induction of at least one of these genes appears to be independent of salsalate's effects on the NF-κB pathway.

3.3. Post-injury administration of salsalate inhibits inflammation-associated morphological changes in microglia/macrophages

To assess the effect of post-CCI administration of salsalate on in vivo activation of sentinel cells, we performed immunofluorescent microscopy analyses of microglia/macrophages at the site of injury at day +7, relative to CCI (we employed Iba1 staining, which does not discriminate between microglia and infiltrating monocytes/macrophages in CCI-injured animals, and we thus refer to these cells as microgia/macrophages). As previously reported (Jin et al., 2012; Wang et al., 2013), CCI induced a clear expansion of Iba1-positive cells in the injury-proximal tissue, with morphological transformation from the typical ramified morphology to the activation-associated ameboid phenotype (Loane and Byrnes, 2010) (Fig. 4A). Importantly, salsalate treatment of injured animals significantly reduced the numbers of activated microglia/macrophages

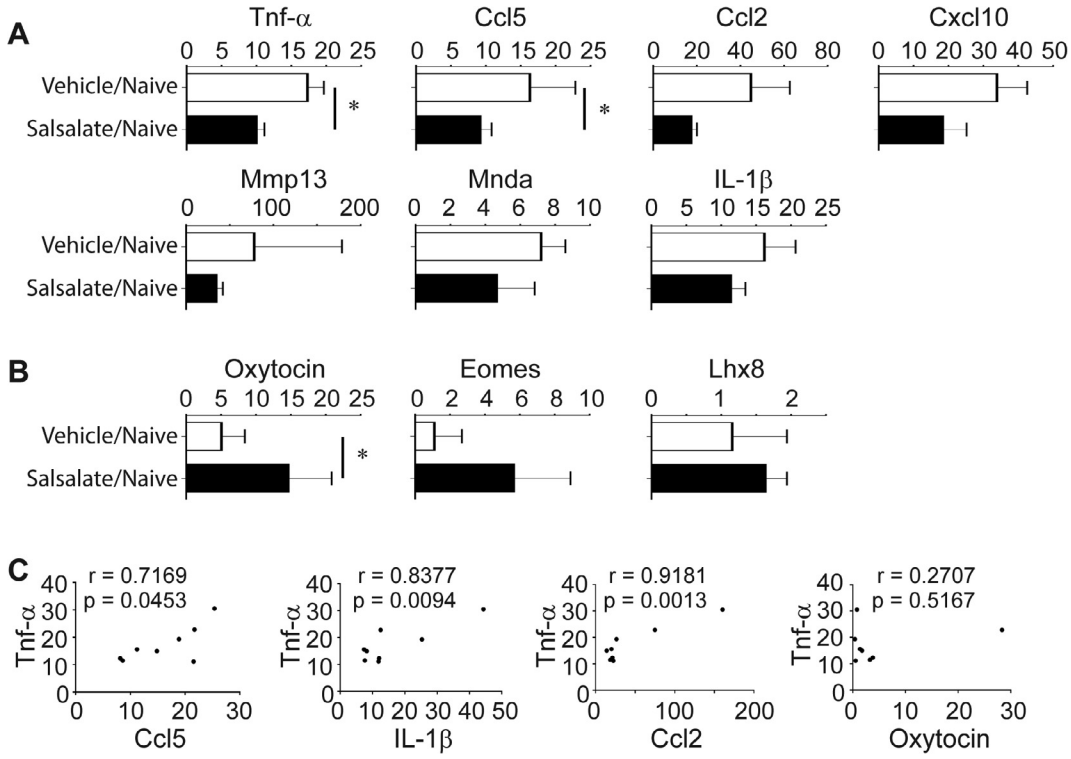

Fig. 3. Real-time PCR analysis of expression of mRNAs identified as differentially expressed by transcriptomics analyses. (A, B) TaqMan RT-PCR validation of (A) seven inflammatory response genes identified as down-regulated by salsalate and (B) three neurogenesis- and neuroprotection-related genes upregulated by salsalate. Values are fold-increase in expression comparing CCI-vehicle (Vehicle) to naïve, and CCI-salsalate (Salsalate) to naïve. $^{*}p < 0.05$, Mann-Whitney *U* test, n = 8. (C) Pearson *r* analysis of correlation between CCI-induced expression of the NF-κB-regulated inflammatory cytokine Tnf-α and three additional inflammatory cytokines (Ccl5, IL-1β, and Ccl2) and the neuropeptide Oxy. n = 8 per group.

at the injury site, as quantified via anti-Iba1 intensity and numbers of microglia/macrophages per section (Fig. 4A–C). Similarly, astrocyte numbers at the injury site increased significantly in response to CCI. Although we found reduced astrocyte expansion in salsalate-treated animals, as measured by reduced GFAP staining intensity and reduced per section numbers of astrocytes (Fig. 4D–F), these reductions were not statistically significant. However, it is notable that in the salsalate treated group, astrocyte numbers and GFAP fluorescence intensity were not statistically different from naïve controls, whereas astrocyte numbers and GFAP fluorescence were significantly elevated in vehicle-treated CCI animals in comparison to naive. Taken together, the data in Fig. 4 show that salsalate significantly diminishes TBI-dependent activation and expansion of microglia/macrophages, with possible attenuation of astrogliosis, as well. In combination with Figs. 2 and 3 data, these observations further confirm that salsalate treatment reduces CCI-induced inflammation.

3.4. Treatment with salsalate alters the kinetics of infiltration and persistence of myeloid cell populations

As the above histological analyses did not discriminate between endogenous microglia and macrophages differentiated from CCI-dependent infiltration of monocytes, we performed a flow cytometry analysis to better define the myeloid populations in the injured brain. Whole brains were processed at day +3 and day +7 relative to CCI to liberate leukocytes, and Percoll-fractionated cells were stained with a panel of antibodies to define discrete myeloid populations (see Materials and Methods for details). Total myeloid cells were defined as the $CD11b^{+}$ population, which represented about 15% of the recovered cells and did not vary significantly across groups (Fig. 5A). However, we did note a trend toward a higher percentage of $CD11b^{+}$ cells at day +3 in the CCI-salsalate group and at day +7 in the CCI-vehicle group. Interestingly, these trends became significant when the gated population was focused on infiltrating myeloid cells, defined as $CD11b^{+}$, $CD45^{high}$. Specifically, the percentage of infiltrating myeloid cells was significantly increased in the day +3 CCI-salsalate group, relative to both naïve and CCI-vehicle. However, by day +7, this population was significantly elevated only in the CCI-vehicle group relative to naïve, whereas the infiltrating myeloid population in the CCI-salsalate group did not significantly differ in comparison to either naïve or CCI-vehicle. By contrast, there was no significant change in the percentage of microglia across treatments, with microglia gated either as $CD11b^{+}$, $CD45^{low}$, or with more precise gating as $CD11b^{+}$, $CD45^{low}$, $Ly6G^{low}$, $Ly6C^{low}$ (Fig. 5A). Thus, the expansion of activated microglia/macrophages observed in the histological analyses may represent a very local expansion not detectable at the level of whole-brain microglia numbers, or it reflects a significant contribution from blood-derived myeloid cells, which cannot be discriminated from microglia based solely on morphology and Iba1 expression.

As the $CD11b^{+}$, $CD45^{high}$ infiltrating myeloid cell population represents a heterogeneous mix of myeloid cells, we also further subdivided this population based on expression of the Ly6G and Ly6C markers. Based on this analysis, we determined that neutrophils ($CD11b^{+}$, $CD45^{high}$, $Ly6G^{high}$, $Ly6C^{low}$) were significantly elevated at Day +3 in the CCI-salsalate group, relative to both naïve and CCI-vehicle (although this was a very rare population across all samples) (Fig. 5A). Additionally, cells meeting an accepted definition of infiltrating inflammatory monocytes ($CD11b^{+}$, $CD45^{high}$, $Ly6G^{low}$, $Ly6C^{high}$) (Szulzewsky et al., 2015) were elevated at day +3 in both the CCI-vehicle and CCI-salsalate groups, relative to naïve. However, by day +7, this population was significantly

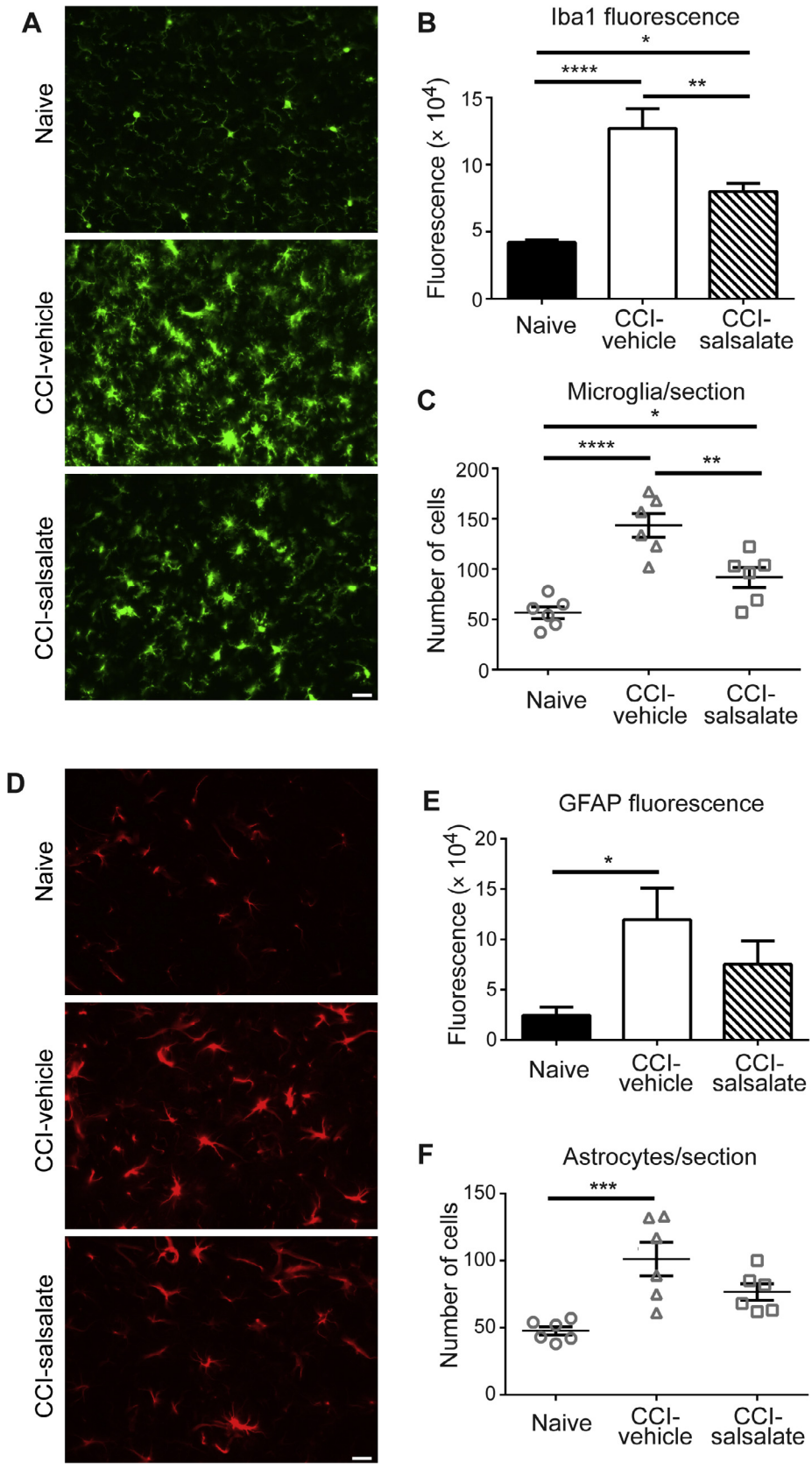

Fig. 4. Salsalate reduces accumulation of activated microglia/macrophages at the site of TBI. (A) Immunofluorescence microscopy images of Iba1 expression in coronal cryosections in a region proximal to the injury site at day +7 relative to CCI. (B,C) Quantification of Iba1 fluorescence intensity (B) and Iba1$^+$ cells (C) in sections from (A). $^{****}p < 0.0001$, $^{**}p < 0.01$, and $^{*}p < 0.05$, one-way ANOVA with Tukey's multiple comparisons test, n = 6 per group. (D) Immunofluorescence microscopy images of GFAP expression in coronal cryosections in a region proximal to the injury site at day +7 relative to CCI. (E,F) Quantification of GFAP fluorescence intensity (E) and GFAP$^+$ cells (F) in sections from (D). $^{***}p < 0.001$ and $^{*}p < 0.05$, one-way ANOVA with Tukey's multiple comparisons test, n = 6 per group.

elevated only in the CCI-vehicle group relative to naïve, with the CCI-salsalate group not differing significantly from either naïve or CCI-vehicle (Fig. 5A–B).

Overall, the above flow cytometry data show that salsalate alters the kinetics of infiltration and persistence of blood derived myeloid cells in the CCI-injured brain, with data suggesting a salsalate-dependent acceleration in clearance of infiltrating myeloid populations by day +7, despite a larger presence of such cells in salsalate-treated animals at day +3. Taken together with the data in Fig. 4, these findings suggest that salsalate modifies the inflammatory response mediated by both injury-site resident microglia and pro-inflammatory myeloid cells that infiltrate from the blood.

3.5. Salsalate treatment following TBI accelerates recovery of motor function

Although the above data demonstrate a clear reduction in local inflammation following TBI, such changes are only of potential clinical relevance if they are correlated with functional recovery. To quantify post-injury functional recovery, we employed two assays of motor function, the rotarod and the beam cross. We have previously shown that motor cortex-targeted CCI induces readily quantifiable changes in motor ability, with progressive recovery of function over the first week post-injury (Lagraoui et al., 2012). To assess the impact of post-CCI salsalate treatment, we measured

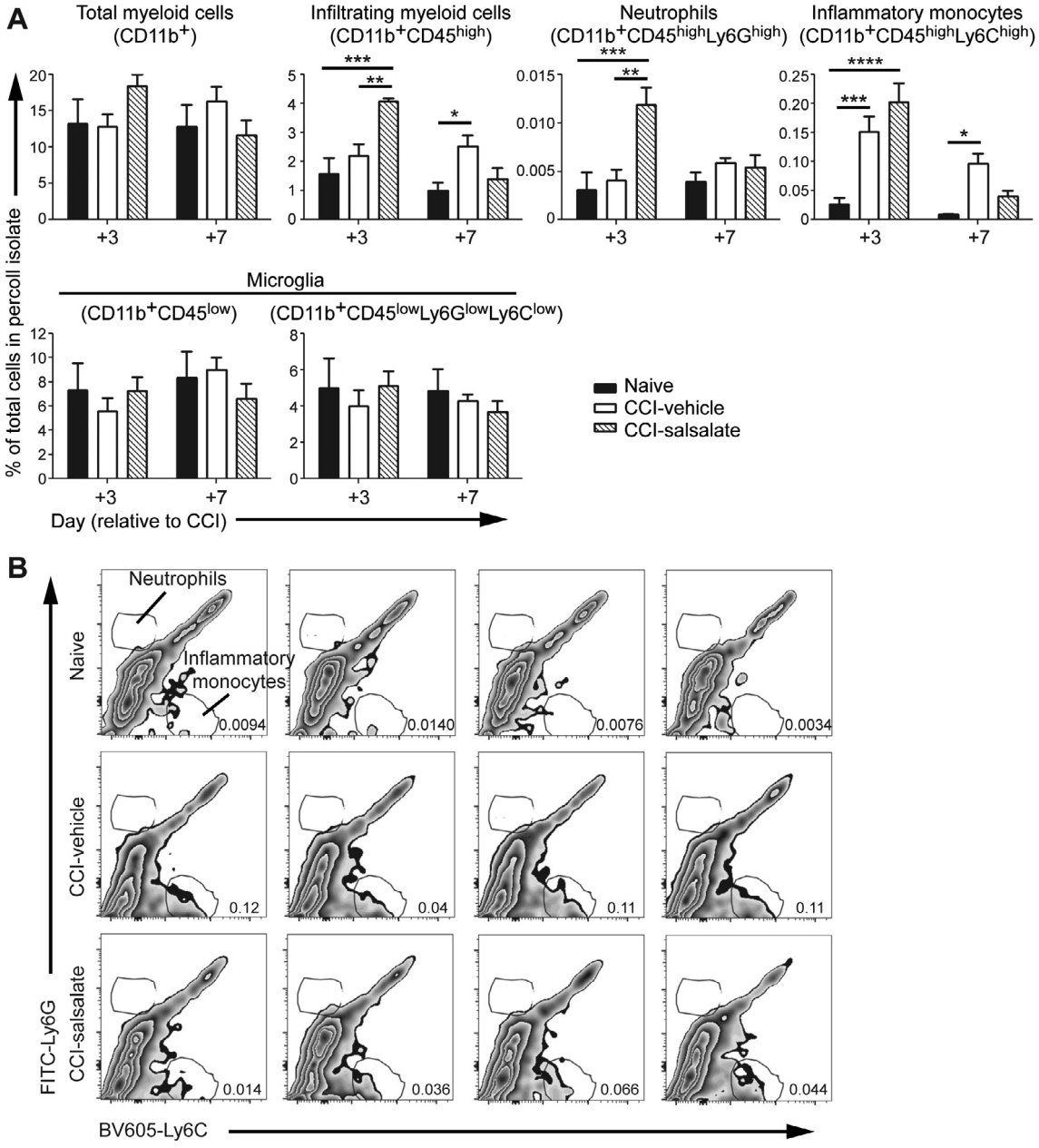

Fig. 5. Salsalate alters the kinetics of infiltration and persistence of blood leukocytes following TBI. Brains were harvested from mice and leukocytes were purified by Percoll gradient fractionation. (A) Quantification of the indicated leukocyte subsets in each treatment group (naïve, CCI-vehicle, CCI-salsalate) at day +3 and day +7 post-CCI, expressed as a percentage of the total live-gated Percoll-purified leukocyte preparation. Markers used to define each subset are indicated for each population. Error bars are SEM. $^{****}p < 0.0001$, $^{***}p < 0.001$, $^{**}p < 0.01$, and $^{*}p < 0.05$, two-way ANOVA with Tukey's multiple comparisons test, n = 4 per group. (B) Primary flow cytometry data on day +7, showing the expression of Ly6C and Ly6G in the $CD11b^{+}$, $CD45^{high}$ (infiltrating myeloid cell) population. Treatment groups are indicated to the left and gates for neutrophils and inflammatory monocytes are identified in the upper left plot. Numbers are quantification of inflammatory monocytes as a percentage of the total live-gated Percoll-purified leukocyte preparation. Numbers are not shown for the neutrophil gate, as there was only a trace population which did not vary between groups.

Table 2
Within-group statistics for rotarod assay.

Rotarod latency to fall			
CCI + vehicle		CCI + salsalate	
Comparison	Significance	Comparison	Significance
D−1 vs. D+1	****	D−1 vs. D+1	ns
D−1 vs. D+3	ns	D−1 vs. D+3	ns
D−1 vs. D+7	ns	D−1 vs. D+7	**
D+1 vs. D+3	*	D+1 vs. D+3	***
D+1 vs. D+7	****	D+1 vs. D+7	****
D+3 vs. D+7	ns	D+3 vs. D+7	ns
Rotarod reached speed			
CCI + vehicle		CCI + salsalate	
Comparison	Significance	Comparison	Significance
D−1 vs. D+1	***	D−1 vs. D+1	ns
D−1 vs. D+3	ns	D−1 vs. D+3	ns
D−1 vs. D+7	ns	D−1 vs. D+7	**
D+1 vs. D+3	ns	D+1 vs. D+3	***
D+1 vs. D+7	****	D+1 vs. D+7	****
D+3 vs. D+7	*	D+3 vs. D+7	ns

**** $p < 0.0001$.
*** $p < 0.001$.
** $p < 0.01$ and.
* $p < 0.05$.

baseline performance at day −1 relative to CCI, and post-injury performance at days +1, +3 and +7. As shown in Table 2, CCI caused a significantly reduced latency to fall and reached speed at day −1 vs. day +1 in vehicle-treated animals, whereas there was no significant change in these parameters in salsalate-treated animals. Additionally, although both groups showed significantly improved performance in at least one of these parameters at day +3 vs. day +1 and at day +7 vs. day +1, only the salsalate-treated group demonstrated significant improvement in performance at day +7 vs. day −1. Furthermore, in the between groups comparison, the rotarod performance in the salsalate-treated group was significantly better than the vehicle-treated group at days +3 and +7 post-CCI (Fig. 6A–B). Moreover, whereas untreated animals did not reach pre-injury performance levels until day +7, salsalate treated animals exceeded pre-injury performance by day +3 (with the improvement being significant by day +7).

In the balance beam assay, the vehicle treated animals required significantly more time to cross the beam on days +1 and +3 vs. day −1, whereas there was no significant difference in beam cross time between day −1 and any other time point for salsalate-treated animals (Table 3). The vehicle-treated animals showed significant recovery in performance between days +1 and +3 and days +1 and +7 (and the salsalate-treated animals did not demonstrate recovery in function in this assay, because there was no significant loss of function in this group). The between-groups comparison reinforced these observations, demonstrating that the salsalate-treated animals performed significantly better in the beam cross time on days +1 and +3.

Analysis of beam cross foot slips data yielded similar findings, with vehicle-treated animals exhibiting more foot-slips on days +1, +3 and +7, relative to day −1, whereas salsalate-treated animals had significantly increased foot-slips only at day +1 vs. day −1. Importantly, salsalate-treated animals exhibited significantly reduced foot slips between day +1 and day +7, recovering to nearly the pre-training performance level. By contrast, the vehicle-treated animals did not exhibit a significant improvement following injury (Table 3). In the between-groups comparison, salsalate-treated animals had significantly fewer foot slips than the vehicle-treated animals on days +3 and +7. Indeed, the untreated animals remained severely impaired by this measure at day +7, making approximately 3× as many foot slips as during the pre-injury measurement (Fig. 6C–D). Finally, in the combined beam cross score, the vehicle treated animals exhibited a significantly increased overall score on days +1 and +3, relative to day −1, whereas there was not a significant change in score for salsalate-treated animals (although the value was very near significant for the salsalate-treated animals on day +1 vs day −1, $p = 0.0533$) (Table 3). In the beam cross score between-groups comparison, salsalate-treated animals scored significantly better than vehicle-treated on day +3 (Fig. 6E). Taken together, these data show that salsalate treatment results in both a significant acceleration of and improvement in functional recovery in the 7 days following CCI injury.

4. Discussion

In this report, we have shown that salsalate treatment following CCI reduced expression of a large number of NF-κB-regulated inflammatory genes and promoted expression of a number of genes which have known neuroprotective and neurogenic activities. Additionally, salsalate diminished accumulation of activated microglia/macrophages (and possibly astrocytes) at the injury site, and it altered the kinetics of accumulation of blood-derived myeloid cells, with an apparent reduction (vs. vehicle treatment) in several distinct myeloid populations by day +7. The above transcriptional and cellular changes correlated with improved recovery of motor function, as assessed by two different behavioral assays. Collectively, these data suggest that salsalate promotes a multifactorial biological response, promoting functional recovery from penetrating TBI.

With respect to the repressed gene set, although reductions were modest, they were consistently observed across numerous inflammatory genes, suggesting a broad suppression of the inflammatory response. It is important to note that the inflammatory response to CCI has a significant variability in magnitude, with a high standard deviation. This high variability made the statistical discrimination of modest effects on gene transcription more challenging in the real-time PCR assay. However, as the effects were always repressive and always consistent with the RNA sequencing data, there is a strong basis for our conclusion that salsalate broadly inhibits the local inflammatory response to CCI. Moreover, the CCI-induced inflammatory genes were highly correlated, suggesting that the effect of salsalate was on a related gene set: specifically the set of genes induced by NF-κB (Lagraoui et al., 2012). Indeed, when comparing the CCI-vehicle group to the CCI-salsalate group, 26 of 28 NF-κB-regulated genes with statistically significant changes were downregulated by salsalate treatment. Overall, these data are highly consistent with the known inhibitory effect of salsalate/salicylate on the NF-κB pathway (Kopp and Ghosh, 1994; Pierce et al., 1996; Yin et al., 1998).

In our examination of the effects of salsalate on inflammation-associated glial responses, we observed a significantly reduced expansion of activated microglia (and/or infiltrating monocytes/-macrophages) at the site of CCI injury, with a possible reduction in numbers of activated astrocytes. Additionally, our flow cytometry analysis of leukocyte populations revealed salsalate-dependent changes in the kinetics of recruitment and/or persistence of specific blood leukocyte populations. At the day +3 and day +7 time points, neutrophils were detected at very low levels, but with significantly increased numbers in the day +3 CCI-salsalate group, relative to both naïve and CCI-vehicle. Studies of blood leukocyte recruitment in TBI have shown that neutrophils are primarily located in meninges proximal to the site of injury, and tend to be found in the parenchyma only at the focal site of injury, if at all (Corps et al., 2015; Soares et al., 1995). As our tissue preps for flow cytometry did not include the meninges, the low representation of

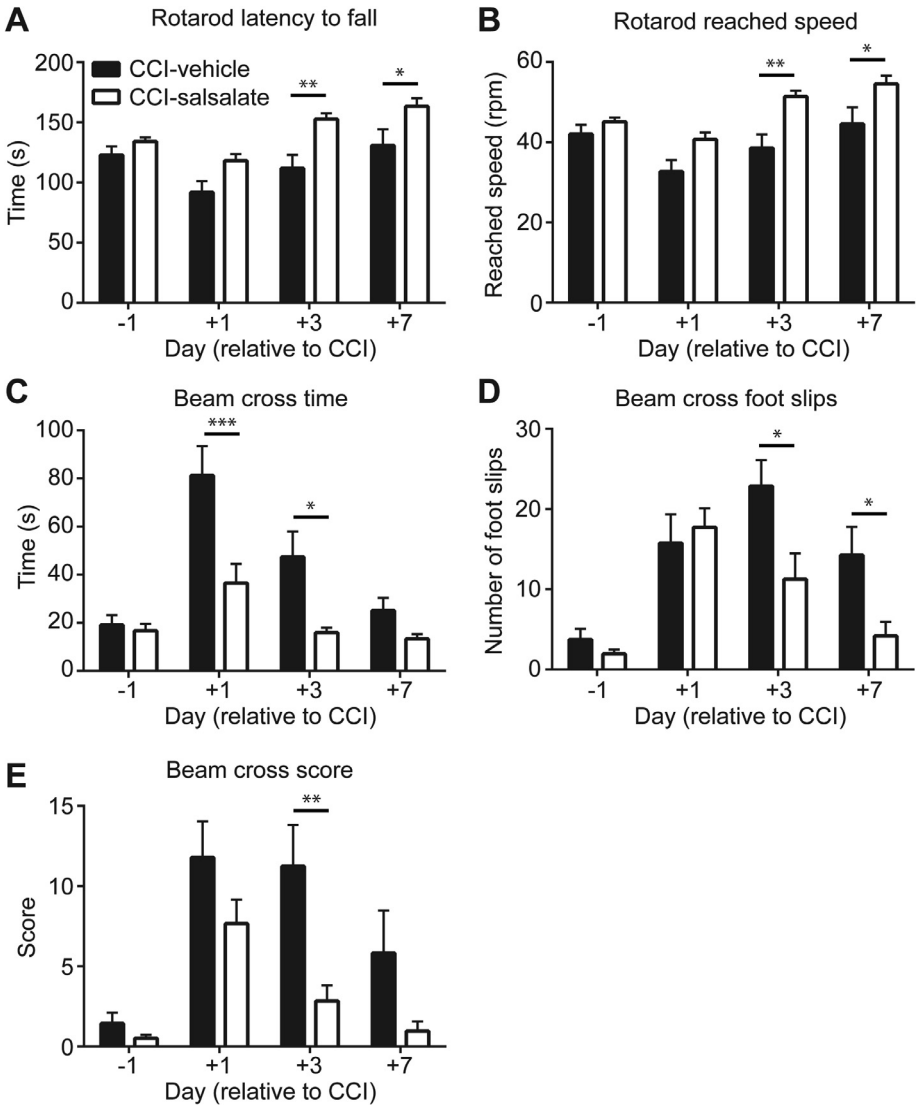

Fig. 6. Post-TBI salsalate treatment results in improved recovery of motor function following TBI. (A, B) Assessment of (A) latency to fall and (B) maximum speed attained on an accelerating rotarod. (C, D, E) Assessment of (C) crossing time latency, (D) number of foot slips and (E) overall score on a balance beam test (see Materials and Methods). $^{***}p < 0.001$, $^{**}p < 0.01$ and $^{*}p < 0.05$, two-way analysis of variance (ANOVA) with Sidak's multiple comparisons test, n = 9 per group.

neutrophils is not surprising. The significant elevation of neutrophils in the CCI-salsalate group at day +3 may represent enhanced accumulation of this cell type at the injury site, and it may thus be biologically significant, despite the low percentages relative to other subsets. As data suggest that neutrophils can be both neuroprotective and pathologic in the context of TBI (Corps et al., 2015), the impact of enhanced neutrophil presence at day +3 following salsalate treatment will require further investigation.

We also observed a change in the kinetics of persistence of infiltrating myeloid cells in the CCI-salsalate group. Both the broadly defined population of $CD11b^{+}$, $Cd45^{high}$ blood-derived myeloid cells and the more strictly defined $CD11b^{+}$, $CD45^{high}$, $Ly6G^{low}$, $Ly6C^{high}$ infiltrating inflammatory monocytes were significantly elevated (vs. naive) at day +3 in the CCI-vehicle and CCI-salsalate groups. However, by day +7, only the CCI-vehicle group had significant elevations of these populations vs. naive. These data suggest a more rapid resolution of the inflammatory response in salsalate-treated animals. Moreover, in comparing the CCI-salsalate group to CCI-vehicle in our RNA sequencing data and flow cytometry analyses, we observed reduced transcription of inflammatory genes at day +3, despite the significantly increased percentages of infiltrating myeloid cells and neutrophils in the CCI-salsalate group and similar percentages of inflammatory monocytes in both groups. These data suggest that the anti-inflammatory effects of salsalate at day +3 are the result of suppression of inflammatory gene expression without inhibition of recruitment of blood leukocytes. However, by day +7, the recruitment and/or retention of blood leukocytes is diminished by salsalate, presumably as a consequence of repression of inflammatory cytokines, many of which are chemokines.

Although the analysis of microglia by flow cytometry did not reveal significant changes in this cell type at either time point, this is not surprising, as the CCI injury is focal, impacting microglia populations only in the injury-proximal region of the brain parenchyma. Thus, changes in resident microglia numbers were detectable by histological examination of the local injury site, but not by flow cytometry analysis of the leukocyte content of the entire brain.

Overall, our data show that salsalate suppresses the injury-induced inflammatory response at both the gene expression and cellular levels. Importantly, salsalate mediates the above anti-inflammatory effects without inhibition of the clotting cascade (Sweeney and Hoernig, 1991). In contrast to aspirin and most

Table 3
Within-group statistics for beam cross assay.

Beam cross time			
CCI + vehicle		CCI + salsalate	
Comparison	Significance	Comparison	Significance
D−1 vs. D+1	****	D−1 vs. D+1	ns
D−1 vs. D+3	**	D−1 vs. D+3	ns
D−1 vs. D+7	ns	D−1 vs. D+7	ns
D+1 vs. D+3	**	D+1 vs. D+3	ns
D+1 vs. D+7	****	D+1 vs. D+7	ns
D+3 vs. D+7	ns	D+3 vs. D+7	ns
Beam cross foot slips			
CCI + vehicle		CCI + salsalate	
Comparison	Significance	Comparison	Significance
D−1 vs. D+1	*	D−1 vs. D+1	**
D−1 vs. D+3	****	D−1 vs. D+3	ns
D−1 vs. D+7	*	D−1 vs. D+7	ns
D+1 vs. D+3	ns	D+1 vs. D+3	ns
D+1 vs. D+7	ns	D+1 vs. D+7	**
D+3 vs. D+7	ns	D+3 vs. D+7	ns
Beam cross score			
CCI + vehicle		CCI + salsalate	
Comparison	Significance	Comparison	Significance
D−1 vs. D+1	**	D−1 vs. D+1	ns
D−1 vs. D+3	**	D−1 vs. D+3	ns
D−1 vs. D+7	ns	D−1 vs. D+7	ns
D+1 vs. D+3	ns	D+1 vs. D+3	ns
D+1 vs. D+7	ns	D+1 vs. D+7	ns
D+3 vs. D+7	ns	D+3 vs. D+7	ns

**** $p < 0.0001$.
** $p < 0.01$.
* $p < 0.05$.

NSAIDs, which are potent Cox-1 inhibitors, salsalate has a very high IC_{50} for both Cox-1 and Cox-2 (4956 μM and 482 μM, respectively) (Marnett, 2009). Clearly, the absence of an anticoagulant effect in the context of brain injury is highly desirable, as even minor brain hemorrhage can have catastrophic consequences.

The magnitude of the in vivo reduction of the injury-induced pro-inflammatory program was smaller in comparison to what we observed in our in vitro analyses of microglia responses to LPS stimulation. One key difference between these experiments is that in vitro studies were performed as pre-treatments whereas salsalate administration in vivo was performed 30 min post-injury. Thus, the inflammatory cascade was blocked from the outset in BV2 cells, whereas there was a significant period of initiation of inflammation prior to salsalate exposure in vivo. We also surmise that the concentration of salsalate in the brain may not reach the concentration required for highly effective suppression of inflammation, and/or that the once-per-day administration of this drug results in periods of diminished salicylate concentration in the brain, relaxing the block on NF-κB activation. Significant fluctuations in plasma salicylate concentration do occur in rodents and man over a 16-h period following salsalate ingestion (Cao et al., 2012; Harrison et al., 1981), suggesting that more frequent dosing would be required to maintain a consistent concentration in blood plasma and the CNS parenchyma.

While it is tempting to speculate that better suppression of the inflammatory response would further improve functional outcomes, this may not be the case. Indeed, the inflammatory and post-injury healing response consists of many elements that inhibit CNS neuroregeneration (Silver et al., 2015), including the glial scar (Bush et al., 1999; Cafferty et al., 2007; Ridet et al., 1997). However, the inflammatory response is also required for healing of brain injuries; therefore, a complete block of the inflammatory response would be detrimental (Ziebell and Morganti-Kossmann, 2010). Thus, the ideal TBI therapy would preserve the healing aspects of the inflammatory response, while interfering with those activities that inhibit repair and replacement of damaged and dead neurons (Kumar and Loane, 2012). It is intriguing to speculate that the modest inhibition of inflammation by salsalate observed in this study may actually be of more therapeutic benefit than alternative treatments that achieve a stronger blockade of this response. Further comparative studies would be required to definitively address this hypothesis.

Although salsalate/salicylate has been known as an NF-κB inhibitor for more than 20 years, recent work has also identified IKK/NF-κB-independent effects, including activation of adenosine monophosphate-activated protein kinase (AMPK) (Hawley et al., 2012) and inhibition of CBP and p300 lysine acetyltransferase activity (Shirakawa et al., 2016). Moreover, salicylate stimulation of p300 has recently been shown to prevent tau acetylation on lysine 174 and lower total levels of tau in a mouse model of Alzheimer's disease, resulting in functional improvement (Min et al., 2015). As data suggest that tau also has a pathological role in TBI-induced neurodegeneration, particularly in the context of repeated TBI and chronic traumatic encephalophathy (CTE) (Daneshvar et al., 2015; Ojo et al., 2016; Washington et al., 2016), the p300-tau pathway represents another NF-κB-independent target of salsalate, which may further augment functional recovery from TBI. Additionally, salsalate therapy would also suppress the inflammatory response of peripheral immune system, which may lead to therapeutic benefit in TBI associated with polytrauma, which is common in military TBI and motor vehicle accidents. In this regard, there is increasing evidence of a variety of mechanisms by which peripheral immune responses impact CNS function (Marin and Kipnis, 2016). Further investigation will be required to determine if any of the above activities of salsalate contribute to the therapeutic benefit for TBI, reported in this work.

Interestingly, salsalate is currently being explored as a therapy for diabetes and pre-diabetes (Goldfine et al., 2008; Knudsen and Pedersen, 2015). While considerable data suggest that the IKKβ-suppressing anti-inflammatory activity of salsalate is responsible for the therapeutic benefit (Knudsen and Pedersen, 2015; Yuan et al., 2001), this interpretation may be too simplistic, as there are indications that salsalate-mediated AMPK activation is also critical for efficacy in treatment of diabetes (Steinberg et al., 2013). Thus, the success of salsalate as a diabetes therapy may be due to the unique spectrum of diverse biological processes altered by this drug.

In this work, we found that salsalate promotes transcription of numerous genes that are associated with neuroprotection and/or neurogenesis. Among this group of genes were Eomes (also known as Tbr2), a transcription factor required for adult neurogenesis in the dentate gyrus (Hodge et al., 2012); Lhx8, a transcription factor that drives production of interneuron progenitors (Flandin et al., 2011); Dlx5, a transcription factor involved in neurogenesis and positioning of the developing neural crest (McLarren et al., 2003; Perera et al., 2004); Dcx, a key regulator of neuronal migration (Wynshaw-Boris et al., 2010); and Meis2 and Six3, two homeobox transcription factors involved in neurogenesis (Agoston et al., 2014; Appolloni et al., 2008). Additional upregulated genes included the regulators of neuronal development, Frdm7, and the retinoic acid receptor, Rarb (Betts-Henderson et al., 2010; Rataj-Baniowska et al., 2015; Serpente et al., 2005). Other salsalate-induced genes include the dopamine receptors, Drd1a and Drd2, which have been shown to mediate neuroprotection in the context of neurodegenerative pathologies such as Parkinson's disease (Calabresi et al., 2013; Lewis et al., 2006). Although our real-time PCR analysis in Fig 2F failed to show statistically significant elevation of two selected genes from this set (Eomes and Lhx8), the high representation of neurogenesis/neuroprotection-associated factors

in a relatively small gene set (13/81 genes induced by salsalate) suggests that these elevations may be biologically significant.

Among the genes identified as induced by salsalate treatment in our transcriptomics analyses, the neuropeptides Oxy and Trh are particularly intriguing as potential contributors to functional recovery. Oxytocin has been shown to mediate both the "social neuroprotection" effect following stroke and to repress microglia activation in vitro (Karelina et al., 2011). Other recent reports connect oxytocin to peripheral neuroregeneration and wound healing (Gumus et al., 2015; Poutahidis et al., 2013), suggesting possible benefits to healing in the context of CCI injury. Analogs of Trh have been extensively studied in TBI, with benefits shown in many experimental models. Moreover, these Trh mimetics promote diverse activities, including protection from apoptosis, reduction of microglia activation, and increased production of neurotrophic and neuroprotective molecules (Loane et al., 2015). Although control of oxytocin gene expression remains incompletely understood, one of the most studied regulatory elements consist of a variety of hormone receptor binding sites (Burbach et al., 2001; Gainer, 2012). Regulation by NF-κB (either positive or negative) has not been reported, to our knowledge. However, data suggest that the oxytocin promoter is responsive to RARβ (Burbach et al., 2001), one of the transcripts upregulated by salsalate, perhaps suggesting a mechanism whereby salsalate stimulates increased production of the oxytocin mRNA. Interestingly, NF-κB has been reported as a repressor of Trh in the context of LPS injection (de Vries et al., 2016). The induction of Trh may therefore reflect release of NF-κB-mediated suppression by salsalate treatment. Thus, the observed induction of neuroprotective and neurogenesis-associated genes likely reflects effects of salsalate that are both dependent and independent of inhibition of NF-κB.

We also observed upregulation of another neuropeptide, vasopressin (Avp), which is closely linked to Oxy and believed to have arisen by a gene duplication event. Both neuropeptides are expressed by the hypothalamo-neurohypophysial system (Burbach et al., 2001). However, unlike oxytocin, existing data suggest that induction of vasopressin in the context of TBI is detrimental through mechanisms that include disruption of the blood-brain barrier and promotion of cerebral edema (Trabold et al., 2008). However, one study suggests that these negative effects are primarily due to amplification of the inflammatory pathway (Szmydynger-Chodobska et al., 2010). Therefore, as salsalate inhibits inflammation, we expect that vasopressin-mediated induction of inflammatory genes may be ameliorated, thereby negating detrimental effects of upregulation of the Avp gene.

Given the uniform lack of success of clinical trials of TBI therapeutics to date (Maas et al., 2012, 2010), many in the TBI field now argue that multifactorial therapies are required, either in the form of multiple drugs targeting distinct aspects of the pathological response, or single drugs with multiple effects (Loane et al., 2015; Margulies et al., 2009; Stoica et al., 2009; Vink and Nimmo, 2009). However, this strategy has also not yet met with success, as evidenced by failure of a recent clinical trial with progesterone therapy for severe TBI (Skolnick et al., 2014). Thus, it remains unclear which combination of biological activities are required for successful treatment of human TBI. In this regard, salsalate may be a promising candidate for further investigation as a TBI therapy, given diverse effects on suppressing inflammation, promoting transcription of neuroprotective and neurogenic genes, and diminishing acetylation and accumulation of tau.

Conflict of interest

The authors declare no conflict of interest.

Acknowledgments

The authors thank A. Fu and L. Tucker for help with design and execution of TBI surgeries and behavior assays; C. Olsen for statistical consultation; D. McDaniel for help with microscopy analyses; and A. Kashyap and C. Huaman for excellent technical assistance. This work was supported by grants from the Center for Neuroscience and Regenerative Medicine and the NIH (GM109887) to B.C.S. The opinions or assertions contained herein are the private ones of the authors and are not to be construed as official or reflecting the views of the Department of Defense, the Uniformed Services University or any other agency of the U.S. Government. The authors declare no competing financial interests.

References

Agoston, Z., Heine, P., Brill, M.S., Grebbin, B.M., Hau, A.C., Kallenborn-Gerhardt, W., Schramm, J., Gotz, M., Schulte, D., 2014. Meis2 is a Pax6 co-factor in neurogenesis and dopaminergic periglomerular fate specification in the adult olfactory bulb. Development 141, 28–38.

Appolloni, I., Calzolari, F., Corte, G., Perris, R., Malatesta, P., 2008. Six3 controls the neural progenitor status in the murine CNS. Cereb. Cortex 18, 553–562.

Betts-Henderson, J., Bartesaghi, S., Crosier, M., Lindsay, S., Chen, H.L., Salomoni, P., Gottlob, I., Nicotera, P., 2010. The nystagmus-associated FRMD7 gene regulates neuronal outgrowth and development. Hum. Mol. Genet. 19, 342–351.

Blasi, E., Barluzzi, R., Bocchini, V., Mazzolla, R., Bistoni, F., 1990. Immortalization of murine microglial cells by a v-raf/v-myc carrying retrovirus. J. Neuroimmunol. 27, 229–237.

Burbach, J.P., Luckman, S.M., Murphy, D., Gainer, H., 2001. Gene regulation in the magnocellular hypothalamo-neurohypophysial system. Physiol. Rev. 81, 1197–1267.

Bush, T.G., Puvanachandra, N., Horner, C.H., Polito, A., Ostenfeld, T., Svendsen, C.N., Mucke, L., Johnson, M.H., Sofroniew, M.V., 1999. Leukocyte infiltration, neuronal degeneration, and neurite outgrowth after ablation of scar-forming, reactive astrocytes in adult transgenic mice. Neuron 23, 297–308.

Cafferty, W.B., Yang, S.H., Duffy, P.J., Li, S., Strittmatter, S.M., 2007. Functional axonal regeneration through astrocytic scar genetically modified to digest chondroitin sulfate proteoglycans. J. Neurosci. 27, 2176–2185.

Calabresi, P., Di Filippo, M., Gallina, A., Wang, Y., Stankowski, J.N., Picconi, B., Dawson, V.L., Dawson, T.M., 2013. New synaptic and molecular targets for neuroprotection in Parkinson's disease. Mov. Disord. 28, 51–60.

Cao, Y., DuBois, D.C., Almon, R.R., Jusko, W.J., 2012. Pharmacokinetics of salsalate and salicylic acid in normal and diabetic rats. Biopharm. Drug Dispos. 33, 285–291.

Chomczynski, P., Sacchi, N., 1987. Single-step method of RNA isolation by acid guanidinium thiocyanate-phenol-chloroform extraction. Anal. Biochem. 162, 156–159.

Corps, K.N., Roth, T.L., McGavern, D.B., 2015. Inflammation and neuroprotection in traumatic brain injury. JAMA Neurol. 72, 355–362.

Daneshvar, D.H., Goldstein, L.E., Kiernan, P.T., Stein, T.D., McKee, A.C., 2015. Post-traumatic neurodegeneration and chronic traumatic encephalopathy. Mol. Cell. Neurosci. 66, 81–90.

de Vries, E.M., Nagel, S., Haenold, R., Sundaram, S.M., Pfrieger, F.W., Fliers, E., Heuer, H., Boelen, A., 2016. The role of hypothalamic NF-kappaB signaling in the response of the HPT-axis to acute inflammation in female mice. Endocrinology 157, 2947–2956.

DeLegge, M.H., Smoke, A., 2008. Neurodegeneration and inflammation. Nutr. Clin. Pract. 23, 35–41.

Faden, A.I., Loane, D.J., 2015. Chronic neurodegeneration after traumatic brain injury: Alzheimer disease, chronic traumatic encephalopathy, or persistent neuroinflammation? Neurotherapeutics 12, 143–150.

Flandin, P., Zhao, Y., Vogt, D., Jeong, J., Long, J., Potter, G., Westphal, H., Rubenstein, J. L., 2011. Lhx6 and Lhx8 coordinately induce neuronal expression of Shh that controls the generation of interneuron progenitors. Neuron 70, 939–950.

Fu, T.S., Jing, R., McFaull, S.R., Cusimano, M.D., 2016. Health & economic burden of traumatic brain injury in the emergency department. Can. J. Neurol. Sci. 43, 238–247.

Gainer, H., 2012. Cell-type specific expression of oxytocin and vasopressin genes: an experimental odyssey. J. Neuroendocrinol. 24, 528–538.

Goldfine, A.B., Silver, R., Aldhahi, W., Cai, D., Tatro, E., Lee, J., Shoelson, S.E., 2008. Use of salsalate to target inflammation in the treatment of insulin resistance and type 2 diabetes. Clin. Transl. Sci. 1, 36–43.

Gorina, R., Font-Nieves, M., Marquez-Kisinousky, L., Santalucia, T., Planas, A.M., 2011. Astrocyte TLR4 activation induces a proinflammatory environment through the interplay between MyD88-dependent NFkappaB signaling, MAPK, and Jak1/Stat1 pathways. Glia 59, 242–255.

Gumus, B., Kuyucu, E., Erbas, O., Kazimoglu, C., Oltulu, F., Bora, O.A., 2015. Effect of oxytocin administration on nerve recovery in the rat sciatic nerve damage model. J. Orthop. Surg. Res. 10, 161.

Harrison, L.I., Funk, M.L., Re, O.N., Ober, R.E., 1981. Absorption, biotransformation, and pharmacokinetics of salicylsalicylic acid in humans. J. Clin. Pharmacol. 21, 401–404.
Hawley, S.A., Fullerton, M.D., Ross, F.A., Schertzer, J.D., Chevtzoff, C., Walker, K.J., Peggie, M.W., Zibrova, D., Green, K.A., Mustard, K.J., Kemp, B.E., Sakamoto, K., Steinberg, G.R., Hardie, D.G., 2012. The ancient drug salicylate directly activates AMP-activated protein kinase. Science 336, 918–922.
Hedner, T., Everts, B., 1998. The early clinical history of salicylates in rheumatology and pain. Clin. Rheumatol. 17, 17–25.
Hellewell, S., Semple, B.D., Morganti-Kossmann, M.C., 2015. Therapies negating neuroinflammation after brain trauma. Brain Res.
Hodge, R.D., Nelson, B.R., Kahoud, R.J., Yang, R., Mussar, K.E., Reiner, S.L., Hevner, R. F., 2012. Tbr2 is essential for hippocampal lineage progression from neural stem cells to intermediate progenitors and neurons. J. Neurosci. 32, 6275–6287.
Jin, X., Ishii, H., Bai, Z., Itokazu, T., Yamashita, T., 2012. Temporal changes in cell marker expression and cellular infiltration in a controlled cortical impact model in adult male C57BL/6 mice. PLoS One 7, e41892.
Karelina, K., Stuller, K.A., Jarrett, B., Zhang, N., Wells, J., Norman, G.J., DeVries, A.C., 2011. Oxytocin mediates social neuroprotection after cerebral ischemia. Stroke 42, 3606–3611.
Karve, I.P., Taylor, J.M., Crack, P.J., 2016. The contribution of astrocytes and microglia to traumatic brain injury. Br. J. Pharmacol. 173, 692–702.
Kettenmann, H., Hanisch, U.K., Noda, M., Verkhratsky, A., 2011. Physiology of microglia. Physiol. Rev. 91, 461–553.
Knudsen, S.H., Pedersen, B.K., 2015. Targeting inflammation through a physical active lifestyle and pharmaceuticals for the treatment of type 2 diabetes. Curr. Diab.Rep. 15, 82.
Kopp, E., Ghosh, S., 1994. Inhibition of NF-kappa B by sodium salicylate and aspirin. Science 265, 956–959.
Kumar, A., Loane, D.J., 2012. Neuroinflammation after traumatic brain injury: opportunities for therapeutic intervention. Brain Behav. Immun. 26, 1191–1201.
Lagraoui, M., Latoche, J.R., Cartwright, N.G., Sukumar, G., Dalgard, C.L., Schaefer, B.C., 2012. Controlled cortical impact and craniotomy induce strikingly similar profiles of inflammatory gene expression, but with distinct kinetics. Front. Neurol. 3, 155.
Lewis, M.M., Huang, X., Nichols, D.E., Mailman, R.B., 2006. D1 and functionally selective dopamine agonists as neuroprotective agents in Parkinson's disease. CNS Neurol. Disord.: Drug Targets 5, 345–353.
Loane, D.J., Byrnes, K.R., 2010. Role of microglia in neurotrauma. Neurotherapeutics 7, 366–377.
Loane, D.J., Stoica, B.A., Faden, A.I., 2015. Neuroprotection for traumatic brain injury. Handbook Clin. Neurol. 127, 343–366.
Maas, A.I., Menon, D.K., Lingsma, H.F., Pineda, J.A., Sandel, M.E., Manley, G.T., 2012. Re-orientation of clinical research in traumatic brain injury: report of an international workshop on comparative effectiveness research. J. Neurotrauma 29, 32–46.
Maas, A.I., Roozenbeek, B., Manley, G.T., 2010. Clinical trials in traumatic brain injury: past experience and current developments. Neurotherapeutics 7, 115–126.
Margulies, S., Hicks, R.Combination Therapies for Traumatic Brain Injury Workshop, L, 2009. Combination therapies for traumatic brain injury: prospective considerations. J. Neurotrauma 26, 925–939.
Marin, I.A., Kipnis, J., 2016. Central nervous system: (Immunological) Ivory Tower or Not? Neuropsychopharmacology.
Marnett, L.J., 2009. The COXIB experience: a look in the rearview mirror. Annu. Rev. Pharmacol. Toxicol. 49, 265–290.
McLarren, K.W., Litsiou, A., Streit, A., 2003. DLX5 positions the neural crest and preplacode region at the border of the neural plate. Dev. Biol. 259, 34–47.
Min, S.W., Chen, X., Tracy, T.E., Li, Y., Zhou, Y., Wang, C., Shirakawa, K., Minami, S.S., Defensor, E., Mok, S.A., Sohn, P.D., Schilling, B., Cong, X., Ellerby, L., Gibson, B.W., Johnson, J., Krogan, N., Shamloo, M., Gestwicki, J., Masliah, E., Verdin, E., Gan, L., 2015. Critical role of acetylation in tau-mediated neurodegeneration and cognitive deficits. Nat. Med. 21, 1154–1162.
Ojo, J.O., Mouzon, B.C., Crawford, F., 2016. Repetitive head trauma, chronic traumatic encephalopathy and tau: challenges in translating from mice to men. Exp. Neurol. 275 (Pt 3), 389–404.
Pahl, H.L., 1999. Activators and target genes of Rel/NF-kappaB transcription factors. Oncogene 18, 6853–6866.
Paintlia, M.K., Paintlia, A.S., Singh, A.K., Singh, I., 2013. S-nitrosoglutathione induces ciliary neurotrophic factor expression in astrocytes, which has implications to protect the central nervous system under pathological conditions. J. Biol. Chem. 288, 3831–3843.
Perera, M., Merlo, G.R., Verardo, S., Paleari, L., Corte, G., Levi, G., 2004. Defective neuronogenesis in the absence of Dlx5. Mol. Cell. Neurosci. 25, 153–161.
Pierce, J.W., Read, M.A., Ding, H., Luscinskas, F.W., Collins, T., 1996. Salicylates inhibit I kappa B-alpha phosphorylation, endothelial-leukocyte adhesion molecule expression, and neutrophil transmigration. J. Immunol. 156, 3961–3969.
Poutahidis, T., Kearney, S.M., Levkovich, T., Qi, P., Varian, B.J., Lakritz, J.R., Ibrahim, Y. M., Chatzigiagkos, A., Alm, E.J., Erdman, S.E., 2013. Microbial symbionts accelerate wound healing via the neuropeptide hormone oxytocin. PLoS One 8, e78898.
Qin, L., Wu, X., Block, M.L., Liu, Y., Breese, G.R., Hong, J.S., Knapp, D.J., Crews, F.T., 2007. Systemic LPS causes chronic neuroinflammation and progressive neurodegeneration. Glia 55, 453–462.
Rataj-Baniowska, M., Niewiadomska-Cimicka, A., Paschaki, M., Szyszka-Niagolov, M., Carramolino, L., Torres, M., Dolle, P., Krezel, W., 2015. Retinoic acid receptor beta controls development of striatonigral projection neurons through FGF-dependent and Meis1-dependent mechanisms. J. Neurosci. 35, 14467–14475.
Ridet, J.L., Malhotra, S.K., Privat, A., Gage, F.H., 1997. Reactive astrocytes: cellular and molecular cues to biological function. Trends Neurosci. 20, 570–577.
Serpente, P., Tumpel, S., Ghyselinck, N.B., Niederreither, K., Wiedemann, L.M., Dolle, P., Chambon, P., Krumlauf, R., Gould, A.P., 2005. Direct crossregulation between retinoic acid receptor beta and Hox genes during hindbrain segmentation. Development 132, 503–513.
Shirakawa, K., Wang, L., Man, N., Maksimoska, J., Sorum, A.W., Lim, H.W., Lee, I.S., Shimazu, T., Newman, J.C., Schroder, S., Ott, M., Marmorstein, R., Meier, J., Nimer, S., Verdin, E., 2016. Salicylate, diflunisal and their metabolites inhibit CBP/p300 and exhibit anticancer activity. eLife 5.
Silver, J., Schwab, M.E., Popovich, P.G., 2015. Central nervous system regenerative failure: role of oligodendrocytes, astrocytes, and microglia. Cold Spring Harbor Perspect. Biol. 7, a020602.
Skolnick, B.E., Maas, A.I., Narayan, R.K., van der Hoop, R.G., MacAllister, T., Ward, J.D., Nelson, N.R., Stocchetti, N., Investigators, S.T., 2014. A clinical trial of progesterone for severe traumatic brain injury. N. Engl. J. Med. 371, 2467–2476.
Smith, C., Gentleman, S.M., Leclercq, P.D., Murray, L.S., Griffin, W.S., Graham, D.I., Nicoll, J.A., 2013. The neuroinflammatory response in humans after traumatic brain injury. Neuropathol. Appl. Neurobiol. 39, 654–666.
Soares, H.D., Hicks, R.R., Smith, D., McIntosh, T.K., 1995. Inflammatory leukocytic recruitment and diffuse neuronal degeneration are separate pathological processes resulting from traumatic brain injury. J. Neurosci. 15, 8223–8233.
Sofroniew, M.V., Vinters, H.V., 2010. Astrocytes: biology and pathology. Acta Neuropathol. 119, 7–35.
Steinberg, G.R., Dandapani, M., Hardie, D.G., 2013. AMPK: mediating the metabolic effects of salicylate-based drugs? Trends Endocrinol. Metab. 24, 481–487.
Stoica, B., Byrnes, K., Faden, A.I., 2009. Multifunctional drug treatment in neurotrauma. Neurotherapeutics 6, 14–27.
Sweeney, J.D., Hoernig, L.A., 1991. Hemostatic effects of salsalate in normal subjects and patients with hemophilia A. Thromb. Res. 61, 23–27.
Szmydynger-Chodobska, J., Fox, L.M., Lynch, K.M., Zink, B.J., Chodobski, A., 2010. Vasopressin amplifies the production of proinflammatory mediators in traumatic brain injury. J. Neurotrauma 27, 1449–1461.
Szulzewsky, F., Pelz, A., Feng, X., Synowitz, M., Markovic, D., Langmann, T., Holtman, I.R., Wang, X., Eggen, B.J., Boddeke, H.W., Hambardzumyan, D., Wolf, S.A., Kettenmann, H., 2015. Glioma-associated microglia/macrophages display an expression profile different from M1 and M2 polarization and highly express Gpnmb and Spp1. PLoS One 10, e0116644.
Tay, T.L., Savage, J., Hui, C.W., Bisht, K., Tremblay, M.E., 2016. Microglia across the lifespan: from origin to function in brain development, plasticity and cognition. J. Physiol.
Trabold, R., Krieg, S., Scholler, K., Plesnila, N., 2008. Role of vasopressin V(1a) and V2 receptors for the development of secondary brain damage after traumatic brain injury in mice. J. Neurotrauma 25, 1459–1465.
Vallabhapurapu, S., Karin, M., 2009. Regulation and function of NF-kappaB transcription factors in the immune system. Annu. Rev. Immunol. 27, 693–733.
Vink, R., Nimmo, A.J., 2009. Multifunctional drugs for head injury. Neurotherapeutics 6, 28–42.
Wang, G., Zhang, J., Hu, X., Zhang, L., Mao, L., Jiang, X., Liou, A.K., Leak, R.K., Gao, Y., Chen, J., 2013. Microglia/macrophage polarization dynamics in white matter after traumatic brain injury. J. Cereb. Blood Flow Metab. 33, 1864–1874.
Washington, P.M., Villapol, S., Burns, M.P., 2016. Polypathology and dementia after brain trauma: does brain injury trigger distinct neurodegenerative diseases, or should they be classified together as traumatic encephalopathy? Exp. Neurol. 275 (Pt 3), 381–388.
Wynshaw-Boris, A., Pramparo, T., Youn, Y.H., Hirotsune, S., 2010. Lissencephaly: mechanistic insights from animal models and potential therapeutic strategies. Semin. Cell Dev. Biol. 21, 823–830.
Yin, M.J., Yamamoto, Y., Gaynor, R.B., 1998. The anti-inflammatory agents aspirin and salicylate inhibit the activity of I(kappa)B kinase-beta. Nature 396, 77–80.
Yuan, M., Konstantopoulos, N., Lee, J., Hansen, L., Li, Z.W., Karin, M., Shoelson, S.E., 2001. Reversal of obesity- and diet-induced insulin resistance with salicylates or targeted disruption of Ikkbeta. Science 293, 1673–1677.
Zamanian, J.L., Xu, L., Foo, L.C., Nouri, N., Zhou, L., Giffard, R.G., Barres, B.A., 2012. Genomic analysis of reactive astrogliosis. J. Neurosci. 32, 6391–6410.
Ziebell, J.M., Morganti-Kossmann, M.C., 2010. Involvement of pro- and anti-inflammatory cytokines and chemokines in the pathophysiology of traumatic brain injury. Neurotherapeutics 7, 22–30.